RESEARCH STATEMENT

YIMIN ZHONG

My general research interests lie in numerical analysis and scientific computing, including numerical solutions of PDEs, numerical optimization, fast algorithms, and applications in inverse problems and imaging science.

1. Overview of Recent Research

My PhD thesis work focuses on numerical analysis of inverse problems in hybrid imaging modalities such as photo-acoustic tomography (PAT) and thermo-acoustic tomography (TAT). These imaging modalities aim at achieving desirable contrast and resolution at the same time. For example, PAT/TAT techniques are based on the fact that time-varying electromagnetic energy could be absorbed and induce acoustic waves (photoacoustic/thermoacoustic effect), when high-energy particles or low-energy radio pulses are delivered into medium of interest (biological tissue), the absorbed energy will be converted into heat, leading to transient thermo-elastic expansion and wide-band ultrasonic emission. The wave signals are finally received by ultrasonic transducers on surface of medium, and then produce images from the collected data, and we are most interested in reconstructing the physical properties of the medium by analyzing the images.

The PAT experiment consists of two separate physical processes at time different scales.

(1) The propagation of high-energy particles in scattering medium which is usually described using radiative transport equation (RTE).
(2) The propagation of ultrasound in heterogeneous medium which is described by the acoustic wave equation.

Due to scale separation, the two processes are only weakly coupled. Image reconstruction in PAT is usually done using a two-step strategy. The first step is formulated as an inverse source problem for the wave equation with known wave speed $c(\mathbf{x})$ [1, 5, 6, 8, 9, 10, 11, 12, 13, 17, 18, 20, 27]. There exists analytic reconstruction when $c(\mathbf{x})$ is constant for certain geometries. If $c(\mathbf{x})$ depends on the spatial variable, there are some iterative time reversal algorithms for this case. The second step is an inverse transport problem where the objective is the reconstruct optical coefficients of heterogeneous media from internal data obtained from the first step [2, 3, 4, 7, 14, 16, 19, 21, 22, 26, 29].

My study focuses on two aspects. The first aspect is on inverse transport problems in PAT. In [22], we analyzed the inverse transport problem in fluorescence PAT. We established uniqueness and stability estimate on the reconstruction and proposed efficient numerical reconstruction methods in various settings. To accelerate numerical inverse transport calculations, we proposed in [23] a fast multipole type algorithm for solving the radiative transport equation. This is believed to be the first algorithm of this type in solving phase space kinetic equations.

The second aspect of my research in PAT is on inverse source problem for the acoustic wave equation. In [24], we studied the problem of unknown ultrasound speed in PAT. We derive some theoretical results on the simultaneous reconstruction of ultrasound speed and optical properties in PAT using data collected from multiple illuminations. In [25], in a simplified setting, we attempt to characterize the uncertainty in the reconstruction of the source function in PAT due to uncertainty in the ultrasound speed. We obtain some stability result and demonstrate the idea with numerical simulations.

The following sections provide slightly more detailed descriptions of my recent research outlined here.

2. Inverse transport problems in fluorescence PAT

In [22], we analyzed inverse transport problems for fluorescence PAT, a variant of PAT for molecular imaging. Fluorescent biochemical markers are injected into biological objects and then will accumulate on target tissues, when excited by external high-energy photons at wavelength λ_x, the markers will also emit near-infrared photons at wavelength λ_m and the particles from external source and markers will cause photo-acoustic phenomenon. Both radiative propagation of particles are described by coupled RTE.

$$
\begin{aligned}
&\mathbf{v}\cdot\nabla u^x(\mathbf{x},\mathbf{v})+\sigma_t^x(\mathbf{x})u^x(\mathbf{x},\mathbf{v})=\sigma_s^x(\mathbf{x})\mathcal{K}(u^x)(\mathbf{x},\mathbf{v}) && \text{in } X,\\
&\mathbf{v}\cdot\nabla u^m(\mathbf{x},\mathbf{v})+\sigma_t^m(\mathbf{x})u^m(\mathbf{x},\mathbf{v})=\sigma_s^m\mathcal{K}(u^m)(\mathbf{x},\mathbf{v})+\eta\sigma_{af}^x(\mathbf{x})\mathcal{I}(u^x)(\mathbf{x}) && \text{in } X,\\
&u^x(\mathbf{x},\mathbf{v})=\mathbf{g}(\mathbf{x},\mathbf{v}),\quad u^m(\mathbf{x},\mathbf{v})=0 && \text{on } \Gamma_-.
\end{aligned}
\tag{1}
$$

where $\sigma_t^x=\sigma_{ai}^x+\sigma_{af}^x+\sigma_s^x$, σ_{ai}^x and σ_{af}^x are absorption coming from intrinsic part and fluorescent markers respectively. $\mathcal{I}(u)$ is the integral of u over angular space $\mathbf{v}\in\mathbb{S}^{d-1}$. η is the quantum efficiency variable of fluorescent markers. Suppose the first step of inverse source problem is solved, we obtain the absorbed energy distribution which comes from two parts. The first part is from external photons, giving $(\sigma_a^x-\eta\sigma_{af}^x)\mathcal{I}(u^x)$ since part of the energy is used for excitation of markers. The second part is from excited marker, which is $\sigma_a^m\mathcal{I}(u^m)$. Our objective is to reconstruct the quantum efficiency η and fluorescence absorption coefficient σ_{af}^x from absorbed energy $H(\mathbf{x})$.

$$
H(\mathbf{x})=(\sigma_a^x-\eta\sigma_{a,f}^x)\mathcal{I}(u^x)+\sigma_a^m\mathcal{I}(u^m)=\sigma_{a,\eta}^x\mathcal{I}(u^x)+\sigma_a^m\mathcal{I}(u^m).
\tag{2}
$$

2.1. Uniqueness of single unknown.

Under certain assumptions on coefficients, we can show that when η is known,

$$
c\|H_1-H_2\|_{L^p}\le\|\eta(\sigma_{1,af}^x-\sigma_{2,af}^x)\mathcal{I}(u^x)\|_{L^p}\le C\|H_1-H_2\|_{L^p},
\tag{3}
$$

when σ_{af}^x is known,

$$
c\|H_1-H_2\|_{L^p}\le\|\sigma_{af}^x(\eta_1-\eta_2)\mathcal{I}(u^x)\|_{L^p}\le C\|H_1-H_2\|_{L^p},
\tag{4}
$$

It is quite straightforward when σ_{af}^x is known and η is not, since the first equation will be completely solvable and nd the second one can be transformed as another RTE with a slightly different scattering kernel

$$
\widetilde{\mathcal{K}}=\frac{\sigma_s^m}{\sigma_t^m}\mathcal{K}+\frac{\sigma_a^m}{\sigma_t^m}.
$$

We can show there is an efficient reconstruction algorithm for this case. On the other hand, when η is known while σ_{af}^x is not, the system will stay coupled and numerical reconstruction could use

an optimization based algorithm, if we consider the problem under linearized setting, we can also derive an explicit reconstruction algorithm.

2.2. **Uniqueness of both unknowns.** Under linearized setting, using $J \geq 2$ datasets, $1 \leq j \leq J$, let $\zeta = \delta(\eta\sigma_{af}^x)$ and $\xi = \delta\sigma_{af}^x$,

$$\mathbf{\Pi}\begin{pmatrix}\zeta\\ \xi\end{pmatrix} = \mathbf{z}, \text{ with } \mathbf{\Pi} = \begin{pmatrix} -I + \Pi_\zeta^1 & I - \Pi_\xi^1 \\ \vdots & \vdots \\ -I + \Pi_\zeta^J & I - \Pi_\xi^J \end{pmatrix} \text{ and } \mathbf{z} = \begin{pmatrix} \frac{H_1'[\eta,\sigma_{af}^x]}{\mathcal{I}(u_1^x)} \\ \vdots \\ \frac{H_j'[\eta,\sigma_{af}^x]}{\mathcal{I}(u_j^x)} \end{pmatrix} \tag{5}$$

where Π_ζ^j and Π_ξ^j are linear operators. However, the system operator on left hand side is (pseudo) invertible only if there exists $1 \leq i < j \leq J$ that $(I-\Pi_\zeta^i)^{-1}(I-\Pi_\xi^j)-(I-\Pi_\zeta^j)^{-1}(I-\Pi_\xi^i)$ is invertible. Numerically, we can adopt Landweber algorithm:

$$\begin{pmatrix}\zeta_{k+1}\\ \xi_{k+1}\end{pmatrix} = (I - \tau\mathbf{\Pi}^*\mathbf{\Pi})\begin{pmatrix}\zeta_k\\ \xi_k\end{pmatrix} + \tau\mathbf{\Pi}^*\mathbf{z} \tag{6}$$

For nonlinear case, we use optimization based algorithm, minimizing objective functional:

$$\Phi(\eta,\sigma_{af}^x) = \frac{1}{2}\sum_{j=1}^{J}\int_\Omega \left(H_j - (\sigma_{a,\eta}^x\mathcal{I}(u^x) + \sigma_a^m\mathcal{I}(u^m))\right)^2 dx + \frac{\beta}{2}\left(\|\nabla\eta\|_{L^2(\Omega)^d} + \|\nabla\sigma_{af}^x\|_{L^2(\Omega)^d}\right) \tag{7}$$

Here we employed LBFGS method to solve the minimization problem.

2.3. **Numerical results.** Following are some of the numerical results based on our algorithms. Noises are added to data by multiply $(1 + \gamma \times 10^{-2}\texttt{normrnd})$ with `normrnd` a standard Gaussian random variable and γ a number representing the noise level in percentage. When $\gamma = 0$, we say the data is noise-free.

- Reconstruction of η, when σ_{af}^x is known.

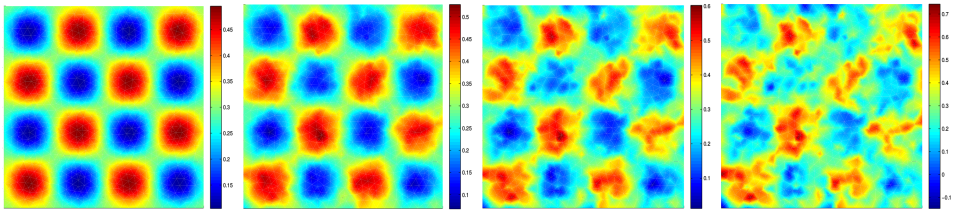

FIGURE 1. The quantum efficiency η reconstructed with different types of data. The noise levels in the data used for the reconstructions, from left to right are $\gamma = 0$, 2, 5 and 10 respectively. The base scattering strength is $\sigma_s^b = 1.0$. The relative L^2 errors in the four reconstructions are 0.01%, 6.42%,16.06% and 32.12% respectively.

- Reconstruction of σ_{af}^x, when η is known.

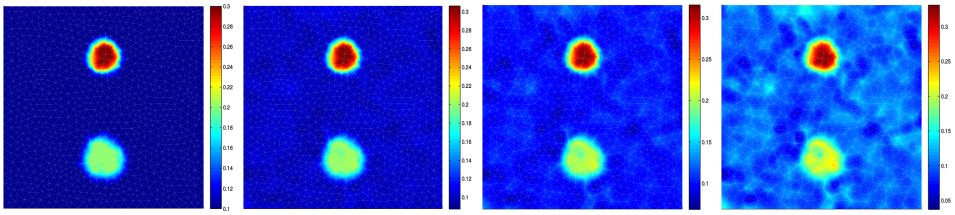

FIGURE 2. The fluorescence absorption coefficient σ_{xf}^a reconstructed with different types of data. The noise level in the data used for the reconstructions, from left to right are: $\gamma = 0$, $\gamma = 2$, $\gamma = 5$, and $\gamma = 10$. The base scattering strength is $\sigma_s^b = 1.0$. The relative L^2 errors are 0.02%,6.70%,16.74% and 33.42%, respectively.

- Reconstruction of both η and σ_{af}^x under nonlinear setting.

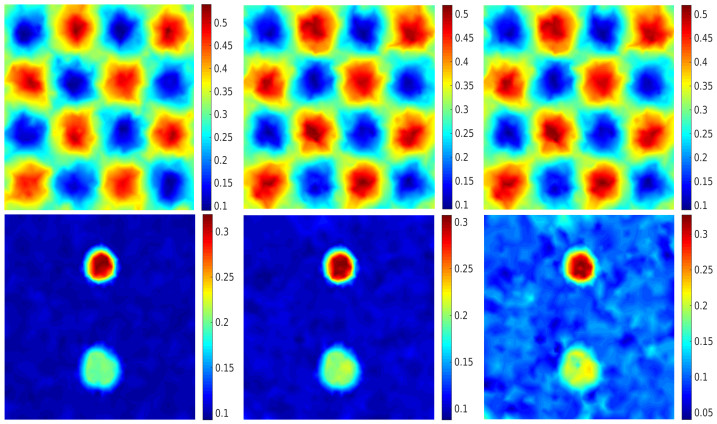

FIGURE 3. Simultaneous reconstruction of the coefficient pair (η, σ_{af}^x) in the nonlinear setting with different types of data. The noise level in the data used for the reconstructions, from left to right, are respectively $\gamma = 0, 1$ and 2. The relative errors in reconstructed (η, σ_{af}^x) are $(16.40\%, 8.32\%), (18.26\%, 9.17\%), (23.26\%, 19.30\%)$ respectively.

3. A FMM-type Algorithm for RTE

Image reconstructions in PAT (and many similar imaging problems, such as optical tomography, fluorescence optical tomography) often requires repeated solutions of the radiative transport equation. In [23], we proposed a fast solver (which is mostly likely going to be used as a preconditioner in more complicated settings) for solving the steady-state RTE in isotropic media. The model we take is:

$$\hat{s} \cdot \nabla \Phi(\vec{r}, \hat{s}) + \mu_t \Phi(\vec{r}, \hat{s}) = \mu_s \fint_{\mathbb{S}^{d-1}} \Phi(\vec{r}, \hat{s}') d\hat{s}' + q(\vec{r}). \tag{8}$$

where $\vec{r} \in \Omega, \hat{s} \in \mathbb{S}^{d-1}$, for simplicity, we assume there is no incoming sources on boundary.

$$\Phi(\vec{r}, \hat{s}) = 0, \quad (\vec{r}, \hat{s}) \in \partial\Omega \times \mathbb{S}^{d-1}, \text{ where } \hat{s} \cdot \hat{n} < 0. \tag{9}$$

here $\hat{n}$ is the external normal vector. Usually RTE solvers, such as those based on the discrete ordinates method, have to discretize angular space $\mathbb{S}^{d-1}$, and will cause severe ray effect if the angular mesh is not fine enough. And if we need very high resolution on unstructured space mesh (triangulation), the unknown variables will be a huge problem for both computing and storage.

3.1. **The main idea.** If we let $f(\vec{r}) = \mu_s \fint_{\mathbb{S}^{d-1}} \Phi(\vec{r}, \hat{s}')d\hat{s}' + q$, we can solve the RTE as

$$\Phi(\vec{r}, \hat{s}) = \int_0^{\tau_-(\vec{r},\hat{s})} \exp\left(-\int_0^t \mu_t(\vec{r} - \nu\hat{s})d\nu\right) f(\vec{r} - t\hat{s})dt. \tag{10}$$

And let $U(\vec{r}) = \fint_{\mathbb{S}^{d-1}} \Phi(\vec{r}, \hat{s}')d\hat{s}'$, and integrate above equation w.r.t angular space $\mathbb{S}^{d-1}$.

$$U(\vec{r}) = \fint_{\mathbb{S}^{d-1}} d\hat{s} \int_0^{\tau_-(\vec{r},\hat{s})} \exp\left(-\int_0^t \mu_t(\vec{r} - \nu\hat{s})d\nu\right) (\mu_s U + q)(\vec{r} - t\hat{s})dt. \tag{11}$$

let $\vec{y} = \vec{r} - t\hat{s}$ in above equation, and define

$$E(\vec{r}, \vec{y}) = \exp\left(-\int_0^t \mu_t(\vec{r} - \nu\hat{s})d\nu\right).$$

$E(\vec{r}, \vec{y})$ describes the total absorption along unit vector $\hat{s}$ from $\vec{r}$ to $\vec{y}$. Under Cartesian coordinate, denote $\nu_{d-1} = \mathrm{Vol}(\mathbb{S}^{d-1})$,

$$U(\vec{r}) = \frac{1}{\nu_{d-1}} \int_\Omega \frac{E(\vec{r}, \vec{y})}{|\vec{r} - \vec{y}|^{d-1}} (\mu_s U + q)(y)dy = K(U + \frac{q}{\mu_s}). \tag{12}$$

where $K : L^2(\Omega) \to L^2(\Omega)$ is a bounded and compact linear operator ($I - K$ is Fredholm). And we can solve U by

$$U = (I - K)^{-1} K \frac{q}{\mu_s}. \tag{13}$$

3.2. **Algorithm based on FMM.** From above analysis, we adopt *kd-tree* for solving the RTE using FMM. The corresponding kernel is

$$K(x, y) = \frac{1}{\nu_{d-1}} \frac{E(x, y)\mu_s(y)}{|x - y|^{d-1}}. \tag{14}$$

And we can approximately compute

$$\phi(x_i) \sim \sum_{j=1}^{N} K(x_i, x_j) \frac{q(x_j)}{\mu_s(x_j)} \tag{15}$$

with $\mathcal{O}(N)$ time cost, even though $E(x, y)$ takes additional time cost, then $U(\vec{r})$ can be computed using Krylov subspace method such as GMRES to solve $(I - K)U = \phi$, each iteration in GMRES will only need $O(N)$ time cost.

3.3. **Numerical results.** The following numerical experiments are taken on Intel i7-3770 CPU of 3.40GHz, 16 Gbytes RAM, Ubuntu 14.04, MATLAB codes are available on Github repository.

- N_p : total number of points in Ω.
- n : number of Chebyshev nodes used.
- s : number of points in each leaf box, here $s = n$.
- T^{FMM} : time cost of FMM evaluation of (15).
- T^{FMM}_{GMRES} : time cost of *GMRES* using FMM solving (13).
- T^{dir} : time cost of direct summation for (15).
- T^{dir}_{GMRES} : time cost of *GMRES* with direct summation solving (13).

N_p	n	$T^{FMM}(s)$	$T^{FMM}_{GMRES}(s)$	$T^{dir}(s)$	$T^{dir}_{GMRES}(s)$	Relative Error
1,024	16	1.20E − 01	3.51E − 02	1.18E + 00	3.71E + 00	2.17E − 04
4,096	16	6.65E − 01	1.25E − 01	4.02E + 01	6.23E + 01	3.39E − 04
16,384	16	3.25E + 00	4.98E − 01	1.09E + 03	9.93E + 02	3.90E − 04
65,536	16	1.50E + 01	2.04E + 00	–	–	–
262,144	16	6.29E + 01	1.00E + 01	–	–	–
1,024	36	2.38E − 01	4.95E − 02	1.18E + 00	3.71E + 00	2.06E − 06
4,096	36	1.38E + 00	1.61E − 01	4.02E + 01	6.23E + 01	3.02E − 06
16,384	36	8.23E + 00	8.83E − 01	1.09E + 03	9.93E + 02	3.18E − 06
65,536	36	3.59E + 01	2.89E + 00	–	–	–
262,144	36	1.59E + 02	1.23E + 01	–	–	–
1024	81	5.43E − 01	1.32E − 01	1.18E + 00	3.71E + 00	9.90E − 16
4096	81	3.64E + 00	5.29E − 01	4.02E + 01	6.23E + 01	4.24E − 09
16,384	81	2.17E + 01	2.80E + 00	1.09E + 03	9.93E + 02	4.47E − 09
65,536	81	1.10E + 02	1.09E + 01	–	–	–
262,144	81	5.76E + 02	4.87E + 01	–	–	–

TABLE 1. Performance for FMM based algorithm in 2D

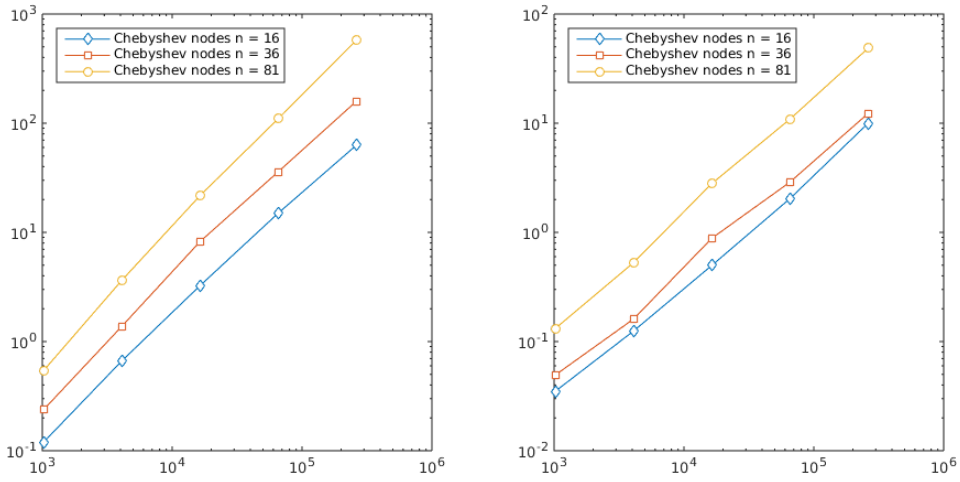

FIGURE 4. Strong scaling for FMM based RTE solver in 2D. Left: T^{FMM}, Right: T^{FMM}_{GMRES}

3.4. **Acceleration Techniques.** Under general setting, the kernel K is not homogeneous nor transitional invariant. Thus SVD pre-computation won't provide any advantages unless the singular values decay very rapidly. Moreover, to accelerate evaluation of $K(x, y)$, we could approximate the line integral $E(x, y)$ by applying FFT on μ_t if it is smooth enough.

4. One Step Reconstruction of both acoustic and optical properties in PAT

When the ultrasound speed is not known, the two-step reconstruction framework in PAT breaks down. In past a few years, there are some results [15, 28] proved that if wave speed is

unknown constant or only depends on a finite number of variables, then wave speed can be uniquely determined. We analyzed the problem simultaneous reconstruction of ultrasound speed and the optical coefficient in [24] where we linearized this model in unit ball and assume wave speed $c(\mathbf{x}) = c_0(\mathbf{x}) + \delta c(\mathbf{x})$, where c_0 is background constant, and $\delta c(\mathbf{x})$ is small perturbation.

$$\begin{aligned} \frac{1}{c^2(\mathbf{x})}\frac{\partial^2 p}{\partial t^2} - \Delta p - (L * p)(t,x) = \frac{1}{c^2(\mathbf{x})}\delta'(t)H(\mathbf{x})\chi_\Omega, \quad \text{in } \mathbb{R}_+ \times \mathbb{R}^d \\ p(t,\mathbf{x}) = 0, \quad \frac{\partial p}{\partial t}(t,\mathbf{x}) = 0, \quad \text{in } \{0\} \times \mathbb{R}^d \end{aligned} \tag{16}$$

where $L(t,x)$ defined as

$$L(t,x) = \frac{1}{\sqrt{2\pi}}\int_{\mathbb{R}} (\mathfrak{R}^2(\omega,\mathbf{x}) - \frac{\omega^2}{c^2}) e^{i\omega t} d\omega \tag{17}$$

Here $\mathfrak{R}$ is the attenuation term, we consider the $\mathfrak{R}$ is in form

$$\mathfrak{R}(\omega,\mathbf{x}) = \frac{\omega}{c} + i\beta|\omega|^\zeta, \ , 1 \le \zeta \le 2. \tag{18}$$

where $\beta(\mathbf{x})$ is spatially varying attenuation coefficient.

4.1. **Uniqueness of $c(\mathbf{x})$ and ill-posedness.** Assuming the medium is not acoustic attenuated (i.e. $\beta \equiv 0$). In one dimensional, we can easily show the uniqueness of wave speed's Fourier coefficients $\mathcal{F}(c)(k)$ if the background pressure field f's Fourier coefficients $\mathcal{F}(f)(2k)$ is non-zero. For higher dimensional cases, to avoid complicated discussion on angular parts, we assume that wave speed is radial, then we conclude similar results that if pressure field f contains certain modes, then wave speed's corresponding modes will be uniquely determined. It is also worth to notice the ill-posedness from integral transforms like Fourier transform or Hankel transform.

4.2. **Stability of $c(\mathbf{x})$ and multiple datasets.** Take three dimensional case for example, let $\widehat{p}_1(\theta,\phi,k)$, $\widehat{p}_2(\theta,\phi,k)$ be transformed measured data where c_1, c_2 are two radial perturbations in wave speed, we can show that

$$\int_0^\infty \left(\frac{d}{dk}(\mathcal{G}(k))\right)^2 dk \ge C\|c_1 - c_2\|^2_{L^2(\Omega)} \tag{19}$$

where

$$\mathcal{G}(k) = \mathrm{Re}\left(\frac{1}{2kh_0^{(1)}(k)}\int_{\mathbb{S}^2} (\widehat{p}_1 - \widehat{p}_2)\sin\theta d\theta d\phi\right) \tag{20}$$

If we consider more general wave speed $c = c(r,\theta,\phi)$, then we will need more datasets, when c has a finite bandwidth in angular spherical decomposition, we could use a finite number of datasets to uniquely determine c. While it is barely possible to reconstruct the exact $c(r,\theta,\phi)$ in practice, because it will require infinite linear independent datasets which is usually not applicable.

4.3. **Uniqueness of acoustic attenuation $\beta(\mathbf{x})$ and more.** In this case, we assume perturbation of wave speed $\delta c \equiv 0$ and β is small enough. In one dimensional, by using multiple datasets (g_1, g_2), we can show that $\mathcal{F}(\beta)(2k)$ can be uniquely determined when the corresponding background pressure fields f_1, f_2 satisfy

$$\mathcal{K}_1^{-1}\mathcal{F}(f_1)(k) - \mathcal{K}_2^{-1}\mathcal{F}(f_2)(k) \ne 0 \tag{21}$$

where $\mathcal{K}_j$ are invertible linear operators w.r.t. appropriate g_j, $1 \leq j \leq 2$. In higher dimension, we can also show similar uniqueness results on radial attenuation coefficients. Furthermore, if we do not impose constraints on the coefficients, we could still show the uniqueness of δc and β by combining the techniques in 4.1 and 4.3.

5. Uncertainty characterization in inverse source problem

In [25], we attempt to analyze in detail the impact of the unknown sound speed on the reconstruction of the source function (i.e. the initial pressure field in PAT). We perform the analysis in a simplified situation where the source is localized (as point sources to be precise). The problem is formulated as: to determine F in the system

$$\begin{aligned} \Delta u(x) + k^2 n(x) u(x) &= F(x). && \text{in } \Omega \\ u &= f(x). && \text{on } \partial\Omega \\ \frac{\partial u}{\partial \mathbf{n}} &= g(x). && \text{on } \partial\Omega \end{aligned} \tag{22}$$

where $\Omega \subset \mathbb{R}^d, d = 2, 3$, $n(x) \in L^2(\Omega)$ is refractive index of the medium, and $n(x)$ has compact support in Ω. The measured data on surface $\partial\Omega$ is $\mathcal{M}(x) = \partial u/\partial \mathbf{n}$. $F(x)$ is linear superposition of point sources that $F(x) = \sum_{i=1}^N h_i \delta(x - x_i)$. $f, g \in L^2(\partial\Omega)$ are measured Cauchy data on surface $\partial\Omega$. The objective is to derive uniqueness and stability for locations of $\{x_i\}_{i=1}^N$ w.r.t Cauchy data (f, g).

5.1. **Uniqueness and stability w.r.t Cauchy data.** If $\{h_i\}_{i=1}^N$ are bounded from below and above by positive real numbers and also point sources are not too close to each other that $\min_{i \neq j} \|x_i - x_j\| = \xi > 0$, then we can show that both of the locations $\{x_i\}_{i=1}^N$ and intensities $\{h_i\}_{i=1}^N$ can be uniquely reconstructed. Following is the stability estimate for $\{x_i\}_{i=1}^N$ w.r.t two datasets (f^1, g^1) and (f^2, g^2).

$$\max_l \min_j \|x_j^1 - x_l^2\| \leq C\xi^{-(N-1)/N} \left(\|g^1 - g^2\| + \|f^1 - f^2\|\right)^{1/N} \tag{23}$$

5.2. **Uniqueness and stability w.r.t** $n(x)$**.** Under the same assumption about locations and intensities of point sources, we can still show that both of the parameter sets can be determined uniquely and give a similar result. Following is the stability estimate for $\{x_i\}_{i=1}^N$ w.r.t refractive index n^1 and n^2.

$$\max_l \min_j \|x_j^1 - x_l^2\| \leq C\xi^{-(N-1)/N} \|n^1 - n^2\|^{1/N} \tag{24}$$

5.3. **Numerical reconstruction.** For numerical experiments, point sources are approximated by thin Gaussian functions in weak sense. The reconstruction results in an optimization problem.

$$\mathbf{x}, \mathbf{h} = \arg\min \int_{\partial\Omega} |f(\mathbf{x}, \mathbf{h}) - \tilde{f}|^2 + |g(\mathbf{x}, \mathbf{h}) - \tilde{g}|^2 \tag{25}$$

where $\tilde{f}, \tilde{g}$ are measured Cauchy data.

6. Future Work

My long term research objective is to develop fast computational algorithms for solving forward and inverse problems related to PDEs. I believe this can only be achieved by combining deep understanding of numerical algorithms with inspiring insights on the PDE/inverse problems (which could only be acquired through extensive numerical and mathematical analysis). I look forward to developing new collaborations in this direction.

My near future research plan is closely related to following problems.

- *Fast algorithms for RTE.* We have mentioned in Section 3 that the FMM algorithm is a promising solver/pre-conditioner for large scale solution of RTE. We plan to analyze in more detail the algorithm for isotropic media and generalize the idea to more complicated settings (for instance, anisotropic media) and systems of RTEs. Moreover, we plan to investigate the efficient usage of the algorithm for solving inverse transport problems in related imaging modalities.
- *Asymptotic numerical reconstruction in one-step framework.* It has been proved that under this framework one could uniquely determine both acoustic and optical properties with multiple measurements, but the reconstruction will be highly unstable unless provided further information/data. We plan to develop stable asymptotic reconstruction schemes for localized (maybe sparse) perturbations in acoustic and optical properties.

References

[1] M. Agranovsky, P. Kuchment, and L. Kunyansky, *On reconstruction formulas and algorithms for the thermoacoustic tomography*, in Photoacoustic Imaging and Spectroscopy, L. V. Wang, ed., CRC Press, 2009, pp. 89–101.

[2] H. Ammari, E. Bossy, V. Jugnon, and H. Kang, *Mathematical modelling in photo-acoustic imaging of small absorbers*, SIAM Rev., 52 (2010), pp. 677–695.

[3] G. Bal and G. Uhlmann, *Inverse diffusion theory of photoacoustics*, Inverse Problems, 26 (2010). 085010.

[4] ———, *Reconstructions of coefficients in scalar second-order elliptic equations from knowledge of their solutions*, Comm. Pure Appl. Math., 66 (2013), pp. 1629–1652.

[5] P. Burgholzer, G. J. Matt, M. Haltmeier, and G. Paltauf, *Exact and approximative imaging methods for photoacoustic tomography using an arbitrary detection surface*, Phys. Rev. E, 75 (2007). 046706.

[6] B. T. Cox, S. R. Arridge, and P. C. Beard, *Photoacoustic tomography with a limited-aperture planar sensor and a reverberant cavity*, Inverse Problems, 23 (2007), pp. S95–S112.

[7] B. T. Cox, T. Tarvainen, and S. R. Arridge, *Multiple illumination quantitative photoacoustic tomography using transport and diffusion models*, in Tomography and Inverse Transport Theory, G. Bal, D. Finch, P. Kuchment, J. Schotland, P. Stefanov, and G. Uhlmann, eds., vol. 559 of Contemporary Mathematics, Amer. Math. Soc., Providence, RI, 2011, pp. 1–12.

[8] D. Finch, M. Haltmeier, and Rakesh, *Inversion of spherical means and the wave equation in even dimensions*, SIAM J. Appl. Math., 68 (2007), pp. 392–412.

[9] M. Haltmeier, T. Schuster, and O. Scherzer, *Filtered backprojection for thermoacoustic computed tomography in spherical geometry*, Math. Methods Appl. Sci., 28 (2005), pp. 1919–1937.

[10] Y. Hristova, *Time reversal in thermoacoustic tomography - an error estimate*, Inverse Problems, 25 (2009). 055008.

[11] A. Kirsch and O. Scherzer, *Simultaneous reconstructions of absorption density and wave speed with photoacoustic measurements*, SIAM J. Appl. Math., 72 (2013), pp. 1508–1523.

[12] P. Kuchment and L. Kunyansky, *Mathematics of thermoacoustic tomography*, Euro. J. Appl. Math., 19 (2008), pp. 191–224.

[13] L. Kunyansky, *Thermoacoustic tomography with detectors on an open curve: an efficient reconstruction algorithm*, Inverse Problems, 24 (2008). 055021.

[14] J. Laufer, B. T. Cox, E. Zhang, and P. Beard, *Quantitative determination of chromophore concentrations from 2d photoacoustic images using a nonlinear model-based inversion scheme*, Applied Optics, 49 (2010), pp. 1219–1233.

[15] H. Liu and G. Uhlmann, *Determining both sound speed and internal source in thermo- and photo-acoustic tomography*, Inverse Problems, 31 (2015). 105005.

[16] A. V. Mamonov and K. Ren, *Quantitative photoacoustic imaging in radiative transport regime*, Comm. Math. Sci., 12 (2014), pp. 201–234.

[17] L. V. Nguyen, *A family of inversion formulas in thermoacoustic tomography*, Inverse Probl. Imaging, 3 (2009), pp. 649–675.

[18] S. K. Patch and O. Scherzer, *Photo- and thermo- acoustic imaging*, Inverse Problems, 23 (2007), pp. S1–S10.

[19] A. Pulkkinen, B. T. Cox, S. R. Arridge, J. P. Kaipio, and T. Tarvainen, *A Bayesian approach to spectral quantitative photoacoustic tomography*, Inverse Problems, 30 (2014). 065012.

[20] J. Qian, P. Stefanov, G. Uhlmann, and H. Zhao, *An efficient Neumann-series based algorithm for thermoacoustic and photoacoustic tomography with variable sound speed*, SIAM J. Imaging Sci., 4 (2011), pp. 850–883.

[21] K. Ren, H. Gao, and H. Zhao, *A hybrid reconstruction method for quantitative photoacoustic imaging*, SIAM J. Imag. Sci., 6 (2013), pp. 32–55.

[22] K. Ren, R. Zhang, and Y. Zhong, *Inverse transport problems in quantitative PAT for molecular imaging*, Inverse Problems, 31 (2015). 125012.

[23] ———, *A FMM-based algorithm for radiative transport in isotropic media*, Preprint, (2016).

[24] K. Ren and Y. Zhong, *Reconstruction of acoustic and optical properties in PAT/TAT with data from multiple illuminations*, Preprint, (2016).

[25] ———, *Recovering point sources in unknown inhomogeneous environments*, Preprint, (2016).

[26] T. Saratoon, T. Tarvainen, B. T. Cox, and S. R. Arridge, *A gradient-based method for quantitative photoacoustic tomography using the radiative transfer equation*, Inverse Problems, 29 (2013). 075006.

[27] P. Stefanov and G. Uhlmann, *Thermoacoustic tomography with variable sound speed*, Inverse Problems, 25 (2009). 075011.

[28] ———, *Recovery of a source term or a speed with one measurement and applications*, Trans. AMS, 365 (2013), pp. 5737–5758.

[29] R. J. Zemp, *Quantitative photoacoustic tomography with multiple optical sources*, Applied Optics, 49 (2010), pp. 3566–3572.

Department of Mathematics, University of Texas at Austin, Austin, Texas, 78712-1202, U.S.A.

E-mail address: yzhong@math.utexas.edu

URL: http://www.ma.utexas.edu/users/yzhong